Symmetric Blends of Complementary Diblock Copolymers: Multiorder Parameter Approach and Monte Carlo Simulations

June Huh, Henk Angerman, and Gerrit ten Brinke*

Laboratory of Polymer Chemistry and Materials Science Center, University of Groningen, Nijenborgh 4, 9747 AG Groningen, The Netherlands

Received November 17, 1995; Revised Manuscript Received June 4, 1996[⊗]

ABSTRACT: Symmetric diblock copolymer blends $A_fB_{1-f}/A_{1-f}B_f$ ($0 \le f \le 0.5$) are theoretically discussed in terms of a multiorder parameter approach and numerically investigated by Monte Carlo simulations. Theoretically, our main result is that below $f \cong 0.3$, but still in the microphase separation region given by $0.21 \le f \le 0.5$, the concentration profiles of the long and short A-blocks as well as the long and short B-blocks are out of phase. Monte Carlo simulations were used to investigate the nature of the phase transition, micro versus macro, as a function of f. Using the canonical ensemble, the microphase separation temperature (MIST) was determined. The macrophase separation temperature (MAST) was studied with the semi-grand-canonical ensemble combined with the histogram extrapolation technique. The phase diagram differs considerably from the theoretical predictions due to the stretching/polarization of the molecules already far above the transition temperature, thus stabilizing the macroscopically homogeneous state. The out-of-phase behavior between the long and short blocks near the critical value $f \cong 0.21$, separating the micro- and macrophase separation regimes, was confirmed by the simulations.

1. Introduction

Technologically important block copolymer systems are often characterized by a distribution in chain length as well as block length. Thermoplastic elastomers consist of multiblock copolymers with alternating soft and hard blocks, where the number of blocks, the block length, and the chain length all vary from polymer to polymer.[1] Theories to deal more accurately with these types of systems have been developed over the past five years. A single order parameter approach was introduced by Fredrickson et al.,[2] who demonstrated the presence of micro- or macro-phase separation depending on the chemical correlations within the polymers. Correlated random copolymers were subsequently studied in more detail in refs 3 and 4. In the last reference, a very general theory developed by Dobrynin and Erukhimovich[5] was applied. This theory is a refinement of the original Leibler description[6] obtained by introducing separate order parameters for each type of molecule present. These order parameters are also called detailed densities. As usual, the Landau free energy is developed in a power series of all order parameters (in principle, infinitely many), and this free energy must be minimized with respect to all these order parameters. At first, this seems a very complicated task, which, however, can be solved by observing that at the spinodal the system becomes critical with respect to one particular linear combination of order parameters. This linear combination is therefore called the strongly fluctuating field, all others being weakly fluctuating fields. The procedure is now to expand the free energy up to fourth order in the strongly fluctuating fields and to such order in the weakly fluctuating fields that the terms in which they occur are at least comparable to this fourth-order contribution. In polydisperse polymer systems characterized by infinitely many order parameters, it is rather difficult to discuss in detail the precise nature of the strongly and weakly fluctuating fields. It is obvious of interest to indicate the additional information that becomes available by this detailed description. For this reason and for simulation technical reasons that will become clear further on, we selected to study a particularly simple system consisting of a symmetric binary melt of diblock copolymers $A_fB_{1-f}/A_{1-f}B_f$.

Already a decade ago, Erukhimovich[7,8] considered this symmetric blend and showed that microphase separation can only occur for $(1 - 1/\sqrt{3}) \le 2f \le 1$, where for symmetry reasons we restrict ourselves to $f \le 0.5$. For smaller values of f, the two components differ so much that at first only a separation into spatially uniform macroscopic phases can occur. Subsequently, these macrophases can then microphase separate. The critical point where the phase transition changes its nature from macroscopic to microscopic is known as Lifshitz point,[9] so that this point represents the connecting point between three distinctive states: the spatially uniform ordered phase, the spatially modulated ordered phase, and the disordered phase. Multicritical behavior of this kind has been explored for polymeric systems theoretically as well as experimentally. Theoretically, Broseta and Fredrickson[10] demonstrated isotropic Lifshitz behavior, i.e. the characteristic wave vector q^* changes continuously from 0 to a finite value, for blends of a block copolymer and a homopolymer by using the random phase approximation. Within the mean-field approach, i.e. neglecting fluctuation effects, they found that for large copolymer content, the vertex function in the RPA equation has its minimum at $q^* \neq 0$, whereas at a small copolymer content the vertex function is a monotonically increasing function. For the same system, Bates and co-workers[11] observed experimentally that the critical exponent at the isotropic Lifshitz point was consistent with that of mean-field Lifshitz behavior.

In recent publications,[12,13] general binary diblock copolymer blends, A_fB_{1-f}/A_gB_{1-g}, were considered at all possible compositions. In ref 13, a detailed phase diagram was calculated using a grand-canonical self-consistent field theory developed in ref 14. In the present paper, we will consider symmetric binary diblock copolymer blends $A_fB_{1-f}/A_{1-f}B_f$ at equal volume fraction 0.5 of both types of block copolymers. In the first section, a theoretical analysis in terms of the four order parameters, describing the concentration profiles of the A- and B-units of block copolymer 1 (A_fB_{1-f}) and

[⊗] Abstract published in *Advance ACS Abstracts,* August 15, 1996.

S0024-9297(95)01715-3 CCC: $12.00 © 1996 American Chemical Society

2 ($A_{1-f}B_f$), respectively, will be given. In this way, interesting information is obtained about the fluctuations, especially near the critical value of f separating the macro- and microphase separation regimes. This information is impossible to obtain by the conventional one-parameter approach.

Additional motivation to study this particular system is due to our desire to compare the theoretical predictions with computer simulations to be performed on the same systems. Binder and co-workers[15,16] have studied in detail microphase separation in diblock copolymer melts by Monte Carlo simulations and compared their results with the predictions of Leibler's theory. Although the results agreed qualitatively, striking differences were found related to the non-Gaussian behavior of the polymer conformations already "above" the microphase separation temperature (MST), i.e. in the homogeneous phase. This behavior is indicative of a stretched or elongated state and since this polarization takes place already in the homogeneous phase, it strongly influences the location of the MST.

To study micro- versus macrophase separation in the symmetric diblock copolymer blends, introduced before, by Monte Carlo simulations, another recent development is of interest. Deutch[17] introduced a simulation technique where a grand-canonical sampling was combined with multiple histogram data evaluation. Subsequently,[18] this technique was applied to *symmetric* homopolymer mixtures to investigate macrophase separation. The symmetry simplifies the simulation procedure considerably, as will be discussed in detail in section 3 dealing with the simulation techniques employed. It is primarily for this reason that we have restricted ourselves in this paper to this particular symmetric diblock copolymer blend.

2. Theoretical Considerations

For the symmetric diblock copolymer blend introduced in the Introduction, the spinodal temperature χ_s can be found with the following Random Phase Approximation (RPA) equations:[6,19]

$$S^{-1}(q^2) = \Gamma(q^2) - 2\chi$$

$$2\chi_s = \underset{q^2}{\text{minimum}}\ \Gamma(q^2) \tag{1}$$

$$\Gamma(q^2) = \frac{\langle g_{AA}\rangle + 2\langle g_{AB}\rangle + \langle g_{BB}\rangle}{\langle g_{AA}\rangle\langle g_{BB}\rangle - \langle g_{AB}\rangle^2}$$

where $S(q)$ is the structure factor. The average $\langle g_{\alpha\beta}\rangle$ should be taken over all different molecule types in the system, with weighting factor proportional to the number of such molecules.[19] In the system under consideration, this means

$$\langle g_{\alpha\beta}\rangle = \frac{1}{2}g^1_{\alpha\beta} + \frac{1}{2}g^2_{\alpha\beta} \tag{2}$$

Here $g^s_{\alpha\beta}$ is the second-order correlation function of a molecule of type $s = 1$ or 2 between monomers of type α and β (both indicate A or B). The superscript denotes the molecule species: 1 stands for A_fB_{1-f}, and 2 for $A_{1-f}B_f$. If N is the total number of monomers per molecule, then in the limit of large N, the correlation functions are given by[6]

$$g^1_{AA}(y) = g^2_{BB}(y) = 2N\frac{e^{-fy} + fy - 1}{y^2}$$

$$g^2_{AA}(y) = g^1_{BB}(y) = 2N\frac{e^{-(1-f)y} + (1-f)y - 1}{y^2} \tag{3}$$

$$g^1_{AB}(y) = g^2_{AB}(y) = N\frac{(1 - e^{-fy})(1 - e^{-(1-f)y})}{y^2}$$

where y is related to q by the following well-known expression (a = bond length):

$$y = \frac{1}{6}Na^2q^2 \tag{4}$$

The above expressions are only valid for q-values corresponding to length scales comparable to the radius of gyration of the molecule, or larger. Since these will turn out to be the relevant length scales, the approximations made in obtaining (3) are justified.

The y-value y^* for which Γ attains its minimum is of great importance. If y^* is equal to zero, the system will exhibit a macrophase separation transition, while if y^* differs from zero, there will be a transition to a microphase, with wavelength inversely proportional to y^*. (However, there are exceptions where a system with $y^* = 0$ will show a microphase separation.[4,5]) In the model under study, the value of y^* depends on the value of f. For $f = 0.5$, the system contains only one kind of molecules (a symmetric diblock). Then macrophase separation is impossible, and hence $y^* > 0$. For $f = 0$, it is a blend of two homopolymers, and clearly $y^* = 0$. At

$$f_c = \frac{1}{2}(1 - 1/\sqrt{3}) \cong 0.211325 \tag{5}$$

there is a change from macrophase separation to microphase separation, which is referred to as a Lifshitz point. For $f < f_c$ we are in the macrophase separation regime where $\Gamma(q)$ is a monotonic increasing function of q, implying $q^* = 0$. The RPA equation (1) reduces to the simple Flory–Huggins expression in the infinite wavelength limit, $q \to 0$. By expanding eq 3 for small y, eq 1 is found to be given by the analytic expression

$$S^{-1}(q \to 0) = \frac{4}{N(1-2f)^2} - 2\chi \tag{6}$$

$$N\chi_s = \frac{2}{(1-2f)^2}$$

Not surprisingly, this equation coincides with the value found from the simple random copolymer theory discussed many years ago.[20] In the microphase separation regime, the spinodal has to be calculated numerically. Figure 1 presents the spinodal. The behavior of $y^{*2} = q^{*2}R_g^2$ and $\lambda^*/R_g = 2\pi/q^*R_g$ as a function of f is given in Figure 2. In the limit $f \downarrow f_c$, $y^* \to 0$ and $\lambda^* \to \infty$, Figures 1 and 2 explicitly demonstrate the existence of an isotropic Lifshitz point at $N\chi = 5.96$ and $f = 0.211325$ for this system.

Usually, the state of a polymer system containing two monomer types A and B is described by the deviation of the A-monomer density from the average value (the B-monomer density follows from incompressibility). However, if more than one molecule species is present,

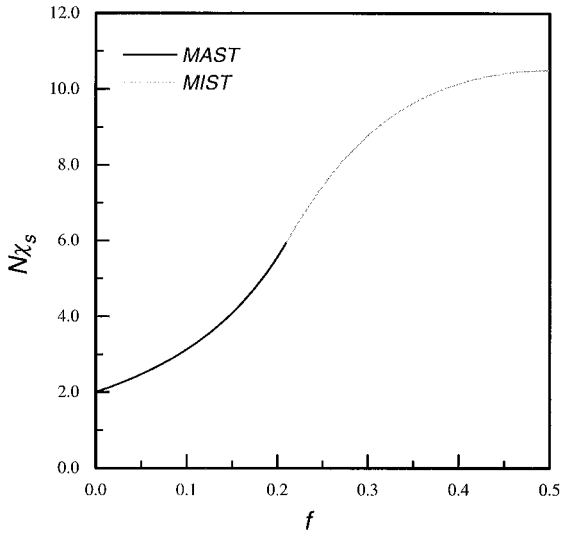

Figure 1. Theoretically predicted spinodal value of $N\chi$ as a function of f for a symmetric diblock copolymer melt $A_fB_{1-f}/A_{1-f}B_f$.

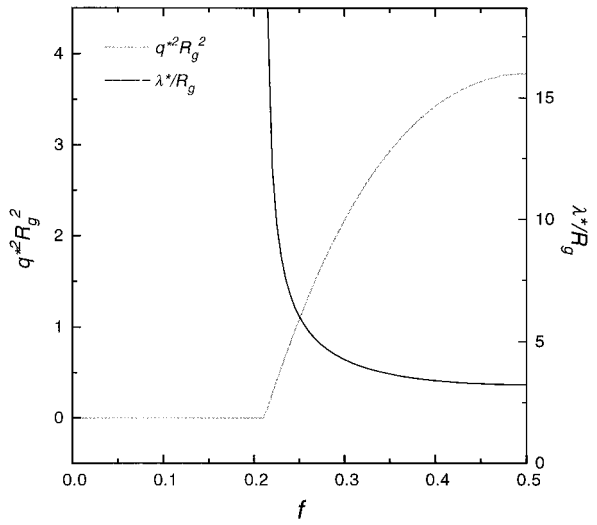

Figure 2. Critical wave vector $q^{*2}R_g^2$ and wavelength λ^*/R_g as a function of f.

a more detailed description can be given by discerning A-monomers belonging to different molecule types.[5] In our model, where two molecule types are present, the state of the system is described by four concentration profiles:

$$\delta\rho_A^1(\bar{r}), \quad \delta\rho_B^1(\bar{r}), \quad \delta\rho_A^2(\bar{r}), \quad \delta\rho_B^2(\bar{r}) \tag{7}$$

where $\delta\rho_A^1(r)$ is the concentration profile of the A-monomers belonging to the molecules of type 1, etc. The total A-monomer concentration profile $\delta\rho_A$ will be the sum of two contributions:

$$\delta\rho_A = \delta\rho_A^1 + \delta\rho_A^2 \tag{8}$$

In our model, $\delta\rho_A^1$ is the profile of the short A-blocks, and $\delta\rho_A^2$ is the profile of the long A-blocks (for $0 < f < 0.5$). In the vicinity of the spinodal, fluctuations with wave vector q^* will be dominant. One particular linear combination of the four different concentration profiles (eq 6) will become critical and is called the strongly fluctuating field. The amplitude of the fluctuations of the separate concentration profiles will be larger for the long A (respectively B) blocks than for the short ones.

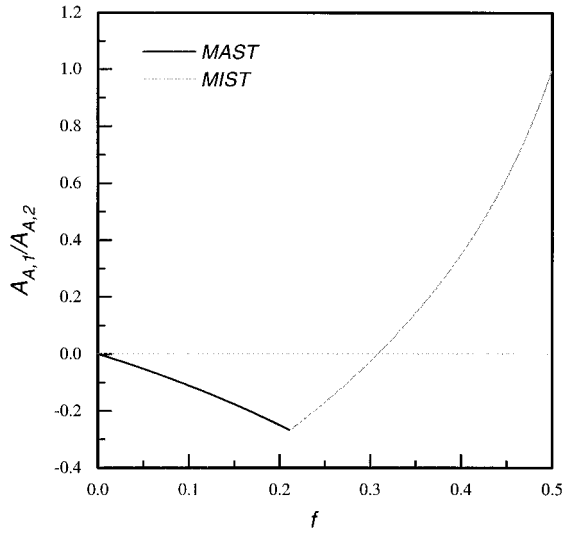

Figure 3. Amplitude ratio (including the phase factor) of the critical concentration fluctuations of A-monomers belonging to the short (subscript A,1) and the long (subscript A,2) A-blocks.

According to ref 5, the ratio between the amplitudes can be calculated from

$$\delta\rho_\alpha^s(q^*) \propto \sum_\beta g_{\alpha\beta}^s(q^*) z_\beta^0(q^*)$$

$$z_\beta^0(q) = \langle g^s\rangle_{\beta A}^{-1}(q) - \langle g^s\rangle_{\beta B}^{-1}(q) \tag{9}$$

The ratio of the amplitudes of the fluctuations of the long A-blocks and the short A-blocks as follows from these expressions is shown in Figure 3. For $f = 0.5$, the blocks are equal and the ratio is 1. Below $f \cong 0.3$, the fluctuations (or, in the phase-separated region, the profiles) of the two A-blocks are out of phase with each other. The long B-blocks so to speak drag the short A-blocks into the B-rich phase. Because the blocks are small, the free energy penalty is small. At $f = 0.211325$, the ratio is equal to the overall ratio (apart from the phase factor -1) $-f/(1-f)$, and macrophase separation sets in.

3. Computational Methodology

As already mentioned in the previous sections, 1:1 molar ratio mixtures of two different types of diblock copolymer 1 and 2 composed of the same segments but of different chemical composition f and $1-f$ (denoted by $A_fB_{1-f}/A_{1-f}B_f$) were investigated by Monte Carlo simulation. Linear self-avoiding copolymer chains with equal chain length, $N = 32$, were generated on a simple cubic lattice with periodic boundary conditions and a small fraction of voids, $\phi_v = 0.2$, was taken to afford chain mobility. An interaction energy between two different segments A and B, ϵ, is assigned whenever A and B segments occupy adjacent sites; all other pairwise interactions are set equal to zero. The chemical composition f of the copolymers is the main system variable varied during the study while other system variables such as the volume fraction of the components, ϕ_i, and the chain length, N, remain constant. To determine the phase transition temperature as a function of f which can correspond either to a macrophase separation transition (MAST) or a microphase separation transition (MIST), we simulated the model system with two different ensembles.

For studying MAST as a function of f, we employed the semi-grand-canonical ensemble combined with the histogram extrapolation technique which was successfully tested for homopolymer blend systems.[18,21,22] Switching identity between copolymers 1 and 2 was performed after some relaxation steps by the slithering snake algorithm[23] to sample the configuration space by the Metropolis importance sampling scheme.[24] For the relaxation of block copolymer chains, the slithering snake model, which resembles the reptation model,[25] turned out to be more efficient for equilibrating the system than other procedures. Particularly for a grand canonical Monte Carlo method, other models using microarrangement of segments connected to two neighboring segments, like bond fluctuation[26] or local kink jump motion,[27] require a large number of canonical trial moves to be performed before a grand canonical step is attempted. The Metropolis transition probability from configuration c to configuration c' for the canonical trial move is given by

$$W(c,c') = \min\{1, e^{-(E'-E)/(k_B T)}\} \tag{10}$$

and for the grand canonical trial move by

$$W(c,c') = \min\{1, e^{\Delta\mu_{12}(\delta'\phi_{12}-\delta\phi_{12})nN/(2k_B T)} e^{-(E'-E)/(k_B T)}\} \tag{11}$$

where E and T are the energy and the temperature of the system, n is the total number of molecules, and $\Delta\mu_{12}$ is the chemical potential difference between copolymer 1 and 2. $\delta\phi_{12}$ is the difference between the volume fraction of copolymer 1 and 2 so that $\delta\phi_{12} = \phi_1 - \phi_2$, which is a key parameter for quantifying macrophase separation. During sampling, we stored a histogram for the variables E and $\delta\phi_{12}$ for the ensemble constants $\{T,\Delta\mu_{12}\}$. Then the probability of $\delta\phi_{12}$ at T and $\Delta\mu_{12}$, $P_{T,\Delta\mu_{12}}(\delta\phi_{12})$, can be approximately estimated by the histogram, $H_{T,\Delta\mu_{12}}(E,\delta\phi_{12})$, recorded for a reasonably large number of independent samplings, n_s:

$$P_{T,\Delta\mu_{12}}(E,\delta\phi_{12}) = \frac{e^{\Delta\mu_{12}\delta\phi_{12}nN/(2k_B T)} e^{-E/(k_B T)} \Gamma(E,\delta\phi_{12})}{Z(T,\Delta\mu_{12})} \approx \frac{H_{T,\Delta\mu_{12}}(E,\delta\phi_{12})}{n_s} \tag{12}$$

$$P_{T,\Delta\mu_{12}}(\delta\phi_{12}) \approx \frac{1}{n_s}\sum_{\{E\}} H_{T,\Delta\mu_{12}}(E,\delta\phi_{12}) \tag{13}$$

where $Z(T,\Delta\mu_{12})$ is the partition function at $\{T,\Delta\mu_{12}\}$ and $\Gamma(E,\delta\phi_{12})$ is the number of configuration with given E and $\delta\phi_{12}$. Subsequently, the probability at a different pair $\{T',\Delta\mu'_{12}\}$, can be obtained by extrapolation from the simulation point, $\{T,\Delta\mu_{12}\}$, provided that $\Gamma(E,\delta\phi_{12})$ is independent of the variables $\{T,\Delta\mu_{12}\}$, by using the following relation:

$$P_{T',\Delta\mu'_{12}}(E,\delta\phi_{12}) = P_{T,\Delta\mu_{12}}(E,\delta\phi_{12}) \times \frac{e^{(\Delta\mu'_{12}-\Delta\mu_{12})\delta\phi_{12}nN/[2k_B(T'-T)]} e^{-E/[k_B(T'-T)]}}{Z(T',\Delta\mu'_{12})/Z(T,\Delta\mu_{12})} \approx \frac{H_{T,\Delta\mu_{12}}(E,\delta\phi_{12}) e^{(\Delta\mu'_{12}-\Delta\mu_{12})\delta\phi_{12}nN/[2k_B(T'-T)]} e^{-E/[k_B(T'-T)]}}{\sum_{\{\delta\phi_{12}\}}\sum_{\{E\}} H_{T,\Delta\mu_{12}}(E,\delta\phi_{12}) e^{(\Delta\mu'_{12}-\Delta\mu_{12})\delta\phi_{12}nN/[2k_B(T'-T)]} e^{-E/[k_B(T'-T)]}} \tag{14}$$

Practically, the simulation point, $\{T,\Delta\mu_{12}\}$, is desired to be at the critical point where the histogram gets sufficiently broad to extrapolate. All simulations for the semi-grand-canonical ensemble were performed in the vicinity of the macrophase separation temperature, T_{MAST}, and at $\Delta\mu_{12} = 0$, noting that the systems simulated here are perfectly symmetric ($A_f B_{1-f}/A_{1-f}B_f$, $N_1 = N_2 = N$) so that the critical chemical potential difference, $\Delta\mu_{12}^c$, is equal to zero (the main reason to concentrate on this particular system).

Canonical systems are also simulated to examine the microphase separation transition. To accelerate the microphase demixing process, the slithering snake algorithm was used and a small fraction of moves consists of interchanging randomly chosen copolymer chains, thus varying the interaction energy but not the composition. For each pair ϵ' ($=\epsilon/k_B T$) and f, 10^4 Monte Carlo steps (MCS) per monomer were attempted to equilibrate the system, and the thermodynamic quantities were subsequently averaged over 100 configurations which were measured every 100 MCS per monomer after the system had reached equilibrium.

4. Monte Carlo Results

In this section, we present our Monte Carlo results and compare them with the theoretical predictions presented in section 2. The systems under consideration have two different modes of concentration fluctuations: the exchange of two different types of copolymer chain 1 and 2, and the polarization between A and B blocks. These two fluctuation modes compete with each other to stabilize either a macrophase- or a microphase-separated structure. The size of these fluctuations is expressed by the scattering intensity, $S(q)$, and the fluctuation mode is observed at $q = 0$ and $q \neq 0$. For a lattice system, this quantity is defined as the Fourier transform of the correlation of the occupation variables:

$$S(\vec{q}) = L^{-3}\langle \sum_{i,j} e^{i\vec{q}\cdot(\vec{r}_i - \vec{r}_j)} \psi(\vec{r}_i)\psi(\vec{r}_j)\rangle \tag{15}$$

$$\psi(\vec{r}) = \phi_B(\vec{r}) - \phi_A(\vec{r}) - (\phi_B - \phi_A) \tag{16}$$

$$\vec{q} = \frac{2\pi}{L}(\nu_1,\nu_2,\nu_3) \tag{17}$$

where $\vec{q}$ and ν_i are the scattering vector and the wavenumber and L is the size of the lattice so that the wavelength $\lambda = 2\pi/q$ becomes $L/|\vec{\nu}|$, preventing that the wavelength becomes larger than the lattice size. The variable $\psi(\vec{r}_i)$ is the order parameter having the values -1, 0, and 1 if the site $\vec{r}_i$ is taken by an A segment, a void, or a B segment, respectively. Because of a small amount of voids, this definition of the order parameter is more relevant than the usual one $\psi(\vec{r}) = \phi_A(\vec{r}) - \phi_A$. The brackets $\langle\ \rangle$ indicate a thermal average. Then $S(\vec{q})$ is spherically averaged over $\vec{q} = |\vec{q}|$ to improve the statistics of the data.

Macrophase Separation. To calculate the scattering intensity of the macro fluctuation mode, $S(q=0)$, we used the semi-grand-canonical ensemble described in the previous section, since the canonical ensemble does not allow its calculation due to the finite lattice size (see eq 17)): Long wavelengths ($q < 2\pi/L$) are cut off in the canonical ensemble. In contrast, using the histogram with respect to $\delta\phi_{12} = \phi_2 - \phi_1$ in the semi-grand-canonical ensemble, the calculation of $S(q=0)$ is quite straightforward. For $q = 0$, eq 15 becomes

$$S(q=0) = L^{-3}\langle[\sum_i \psi(\vec{r}_i)]^2\rangle \quad (18)$$

Observing that the sum of ψ over all lattice sites is equal to $Nn(\phi_B - \phi_A) = Nn(1-2f)\delta\phi_{12}$, where n is the number of polymers, eq 17 becomes

$$S(q=0) = L^{-3}n^2N^2(1-2f)^2 \sum_{\{\delta\phi_{12}\}} \delta\phi_{12}^2 P(\delta\phi_{12}) \quad (19)$$

Then, $S(q=0)$ at different temperatures, $S(q=0,T')$, is found by extrapolation from the temperature simulated:

$$S(q=0,T') \approx \{L^{-3}n^2N^2(1-2f)^2 \sum_{\{\delta\phi_{12}\}} \times \delta\phi_{12}^2 H_{T,\Delta\mu_{12}}(E,\delta\phi_{12}) e^{(\Delta\mu'_{12}-\Delta\mu_{12})\delta\phi_{12}nN/[2k_B(T'-T)]} \times e^{-E/[k_B(T'-T)]}\}/\{\sum_{\{\delta\phi_{12}\}}\sum_{\{E\}} H_{T,\Delta\mu_{12}}(E,\delta\phi_{12}) \times e^{(\Delta\mu'_{12}-\Delta\mu_{12})\delta\phi_{12}nN/[2k_B(T'-T)]} e^{-E/[k_B(T'-T)]}\} \quad (20)$$

Figure 4 presents $S^{-1}(q=0)$ vs $N\epsilon'$ ($=N\epsilon/k_BT$) calculated by the extrapolated histogram from a given simulation point. The plot of $S^{-1}(q=0)$ vs $N\epsilon'$ shows a linear behavior for low values of $N\epsilon'$, where the finite size effect is quite small. For mean-field behavior, $S^{-1}(q=0)$ should be a linear function of ϵ' assuming the Flory–Huggins interaction parameter χ is linear in ϵ':

$$S^{-1}(q=0) = \partial^2 F/\partial\phi_1^2 \propto (\epsilon_c' - \epsilon') \quad (21)$$

where F is the free energy and ϵ_c' is the value of ϵ' at the MAST. To estimate the value of ϵ' at the MAST, we extrapolate the data in the linear region (mean field) to infinite $S(q=0)$. Of course, as reported in several papers,[18,21,28,29] this estimation based on mean field is slightly lower (in terms of ϵ') than the true ϵ_c' due to non-mean-field behavior near the critical region. The size of the non-mean-field region is of the order of N^{-1} so that long chains show mean-field-like behavior. But even for such a small chain as $N = 32$ in our simulations, the difference between mean-field-based $\epsilon'_{c,mf}$ and the true ϵ_c' is less than 5% of the true ϵ_c' which can be determined by finite size scaling.[18,21]

Figure 5 presents the ratio of $\epsilon_c'(f)$ and $\epsilon_c'(0)$ as a function of f as determined in Figure 4. As shown in the theoretical section, our theoretical results for MAST where $f < 0.211325$ turned out to be given by the simple expression

$$\frac{\chi_F^c(f)}{\chi_{eff}^c} = \frac{\chi_F^c(f)}{\chi_F^c(0)} = (2f-1)^{-2} \quad (22)$$

where χ_{eff} is the effective χ-parameter and χ_F is the Flory–Huggins χ-parameter at the macrophase separation transition. This value is comparable to $\epsilon_c'(f)/\epsilon_c'(0)$ if we assume that the prefactor χ/ϵ' is independent of f. Figure 5 shows that the macrophase separation points obtained from the simulations exceed the theoretical results, which indicates that the homogeneous phase is more stable. This trend is more pronounced as f is increased. Within the Flory–Huggins mean-field approach, the local correlation between two monomers is independent of the potential between the monomers. However, in reality, the scale of the interaction potential gives rise to local structure changes propagating to long wavelengths via chain connectivity and leading to changes in $S(q=0)$ and χ_{eff} so that, consequently, χ_{eff}

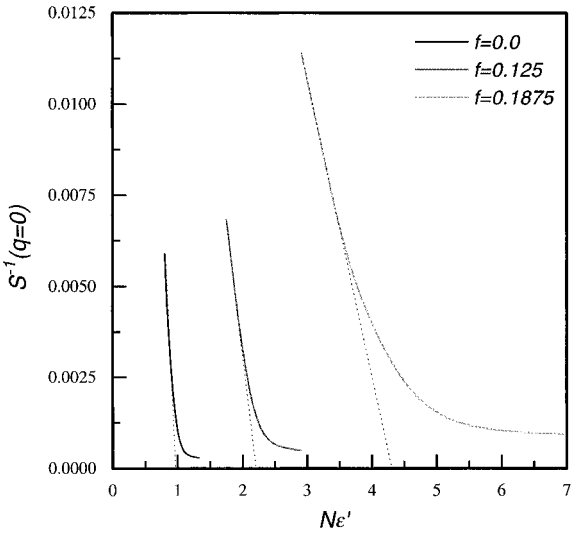

Figure 4. Inverse collective structure factor $S^{-1}(q=0)$ as a function of $N\epsilon'$.

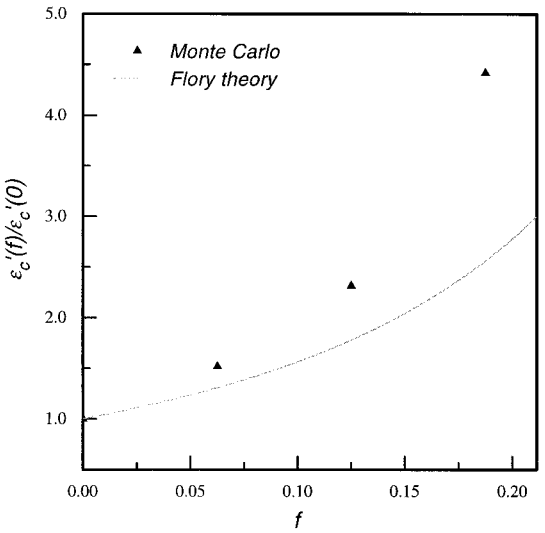

Figure 5. Ratio between the critical macrophase separation interaction energy of the symmetric diblock copolymer blend $A_fB_{1-f}/A_{1-f}B_f$ and the homopolymer blend A/B, $\epsilon_c'(f)/\epsilon_c'(0)$, as a function of f. Solid line represents Flory's theory, and symbols represent computer simulation results.

contains all kinds of nonrandom mixing effects, whereas χ_F is determined by the bare potential, i.e. $\chi_F = (z-2)\epsilon'$. Consequently, due to the local correlations between two interacting monomers induced by local interactions, the mixing process will differ from random mixing and thus eq 22 could be somewhat oversimplified. Recently, the polymer reference interaction site model (PRISM) theory by Curro and Schweizer[30–32] was used to investigate the effect of the local correlations on χ_{eff}/χ_F. They found that the thermally driven local interchain rearrangements lead to the formation of diffuse interfaces and clusters or droplets, leading to χ_{eff}/χ_F being a complicated function of all parameters involved.

To address the issue of the number of different contacts, we start from the mean-field expression of χ_{eff} for the general case of the copolymer blend system A_fB_{1-f}/C_gD_{1-g} given by[20]

$$\chi_{eff} = fg\chi_{AC} + g(1-f)\chi_{BC} + f(1-g)\chi_{AD} + (1-f)(1-g)\chi_{BD} - f(1-f)\chi_{AB} - g(1-g)\chi_{CD} \quad (23)$$

The last two terms on the right-hand side of this

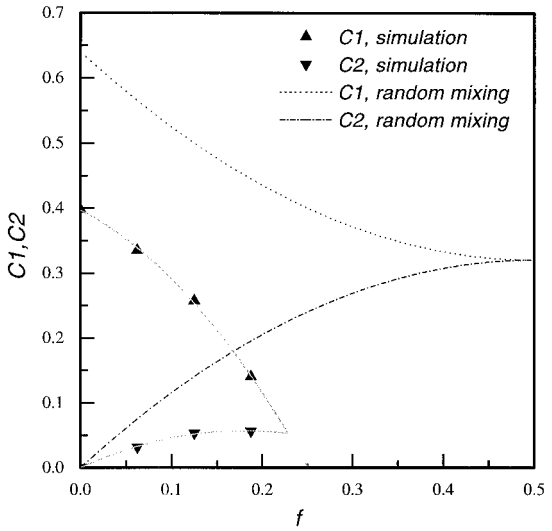

Figure 6. Estimation of unfavorable and favorable part for the random mixing process and the simulation in eq 26 as a function of *f*. C1 represents unfavorable part and C2 represents favorable contribution in enthalpic energy.

equation are often referred to as the "repulsion effect", which act favorably toward mixing in the case of effectively repulsive interactions between the copolymer constituents. Clearly, for our system, eq 23 reduces to

$$\chi_{\text{eff}} = \chi_{\text{AB}}[f^2 + (1-f)^2 - 2f(1-f)] = \chi_{\text{AB}}(1-2f)^2 \tag{24}$$

The terms between the square brackets demonstrate that χ_{eff} consists of two parts: unfavorable contacts between copolymer 1 and copolymer 2 (the first two terms) and the "repulsion effect" between the individual copolymer components. These two terms can be investigated separately by checking unlike contacts during the simulation. The relation is given by

$$\chi_{\text{eff}}\phi_1\phi_2 = \epsilon'(\tilde{n}_{12} + \tilde{n}_{11} + \tilde{n}_{22} - \phi_1\tilde{n}_1^\circ - \phi_2\tilde{n}_2^\circ) \tag{25}$$

where $\tilde{n}_{ij}$ denotes the number of unlike contacts between copolymers *i* and *j per site* and the $\tilde{n}_i^\circ$ denotes the number of unlike contacts in the reference state of pure copolymer *i*. In the mean-field picture, the terms between the square brackets of eq 24 are given by

$$\tilde{n}_{12} = (z-2)\phi_1\phi_2[f^2 + (1-f)^2] \tag{26}$$

$$\phi_1\tilde{n}_1^\circ + \phi_2\tilde{n}_2^\circ - \tilde{n}_{11} - \tilde{n}_{22} = 2(z-2)\phi_1\phi_2 f(1-f)$$

where *z* is the coordination number. In Figure 6, we present these two contributions to χ_{eff} as estimated by the random mixing assumption and as obtained from our simulation. The number of unlike contacts for the simulation was estimated at the MAST. Figure 6 shows that both contributions derived from the simulation results are much lower than the random mixing estimations due to the correlation between interacting sites. The unfavorable, first contribution is much smaller and even of a completely different shape. Apparently, if the asymmetry in the copolymer chains is reduced so that the two different copolymers resemble each other more and more, the polarization between the A- and B-blocks within the different copolymers are in phase with each other, inducing a strong reduction in unfavorable contacts between the two different copolymers. In agreement with this, the second "copolymer repulsion" contribution is also found to be much smaller than the random mixing estimation, but not as much as the former. At high values of *f*, this favorable second contribution is suppressed as a consequence of the low reference energy due to the polarization in the reference state. Unlike contacts between the same copolymer species in the mixture also become smaller by the polarization. Nevertheless, the favorable thermodynamic driving force due to the "repulsion effect" is not so much reduced as the unfavorable first contribution so that an enhanced miscibility for high *f*, compared to the mean-field prediction, is found, even though the phase diagram in Figure 5 was rescaled by ϵ'_c for $f = 0$. In other words, as the system resembles more and more a pure diblock copolymer system, the stretching between the A- and B-blocks of individual diblock copolymer chains or the polarization inside the chains gives rise to an overall polarization between the A- and B-blocks. The polarization between the blocks of the two different copolymer species, which acts favorably on χ_{eff}, is much more sensitive to *f* than the polarization between the blocks of the same copolymer species.

It is difficult to quantify "polarization" more explicitly because it is a collective property. Instead, "stretching" between A- and B-blocks of each copolymer is an intrinsic property of the copolymer itself, different from the collective property of "polarization" but related to it. To investigate the conformational behavior, we have examined conformational quantities such as the root mean square radius of gyration, R_g, and the root mean square distance between the centers of mass of blocks A and B, R_{AB}.

$$R_g = \langle r_g^2\rangle^{1/2} = \left[\frac{1}{nN}\langle\sum_{i=1}^{n}\sum_{j=1}^{N}(\vec{r}_{ij} - \vec{r}_{i,\text{CM}})^2\rangle\right]^{1/2} \tag{27}$$

$$R_{\text{AB}} = \langle r_{\text{AB}}^2\rangle^{1/2} = \left[\frac{1}{n}\langle\sum_{i=1}^{n}(\vec{r}^{\,\text{A}}_{i,\text{CM}} - \vec{r}^{\,\text{B}}_{i,\text{CM}})^2\rangle\right]^{1/2} \tag{28}$$

where $\vec{r}_{ij}$ are the coordinates of the *j*th segment in the *i*th chain and $\vec{r}_{i,\text{CM}}$ and $\vec{r}^{\,\text{k}}_{i,\text{CM}}$ denote the coordinates of the center of mass of the *i*th chain, for the whole chain respectively for the indicated blocks. Using these quantities, we define the degrees of expansion relative to the athermal state by

$$\alpha_g(\epsilon') = R_g(\epsilon')/R_g(\epsilon' = 0) \tag{29}$$

$$\alpha_{\text{AB}}(\epsilon') = R_{\text{AB}}(\epsilon')/R_{\text{AB}}(\epsilon' = 0) \tag{30}$$

Figure 7 shows α_g and α_{AB} as a function of $N\epsilon'$ for $f = 0.1875$. The value of α_g shows a slight decrease up to $N\epsilon' \cong 2$ and then slowly starts to increase to return to the athermal state value as the system approaches the macrophase separation transition. The recovering of the value of α_g has two possible reasons, the stretching of the coil and the formation of a macrophase as the interaction parameter increases. In comparison with α_g, the value of α_{AB} increases rapidly from $N\epsilon' \cong 1$, which demonstrates that the chains already start to stretch well below the MAST.

Microphase Separation. For $f > 0.211325$, where the microphase separation transition (MIST) takes place, we simulated the system by the canonical Monte Carlo method since it requires a huge amount of memory to calculate $S(q,\phi_1)$ by a grand canonical MC method. The interval between two successive grand

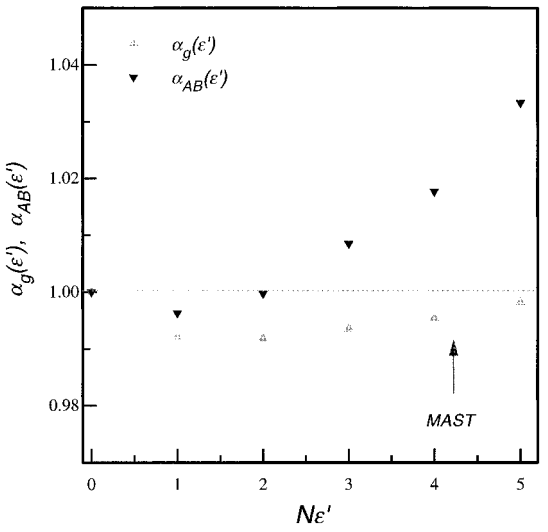

Figure 7. Expansion factors α_g and α_{AB} as a function of $N\epsilon'$ for $f = 0.1875$.

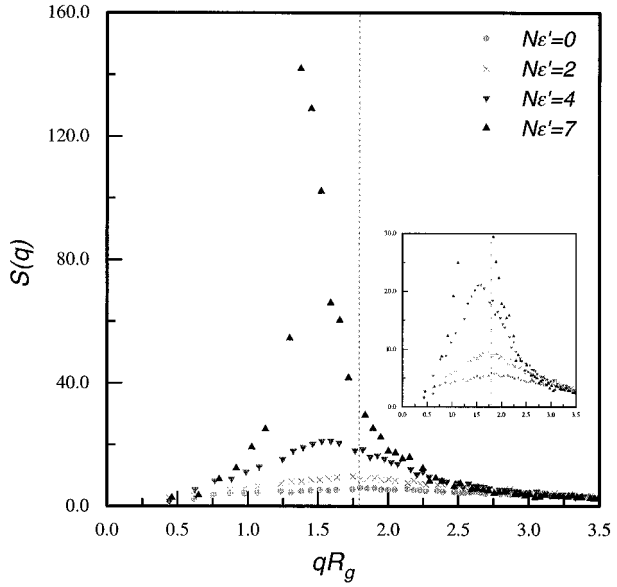

Figure 8. Structure factor $S(q)$ as a function of qR_g for $f = 0.375$ and different values of $N\epsilon'$. Dashed line represents q^*R_g value according to RPA. Inset shows an enhanced vertical scale to more clearly indicate peak position in the low-energy results.

canonical trials has to be equivalent to the relaxation time of the microphase structure so that the computing time is enormously long. Figures 8 and 9 present the collective structure factor as a function of the scaling parameter qR_g for different values of $N\epsilon'$. To overcome the difficulties due to the finite size of the lattice, we investigated with a lattice size $L = 40$ so that the periodicities for the systems simulated are smaller than $L/2$. The peak positions q^*R_g in the plots of Figures 8 and 9 show reasonably good agreement with the estimation by RPA for the athermal state. It is noteworthy that, unlike in pure diblock copolymer systems, the quantity q^*R_g decreases as the asymmetry of a diblock copolymer increases. This is qualitatively comparable with the RPA prediction. However, as $N\epsilon'$ increases, a slight shift of q^*R_g toward smaller values is observed as has been reported before for pure diblock copolymers.[16,33] From our simulation results, the wavelength, $\lambda^* = 2\pi/q^*$, is observed at $4.5R_g$ for $f = 0.375$ and at $5.0R_g$ for $f = 0.3125$, while RPA predicts $3.51R_g$ and $4.07R_g$, respectively.

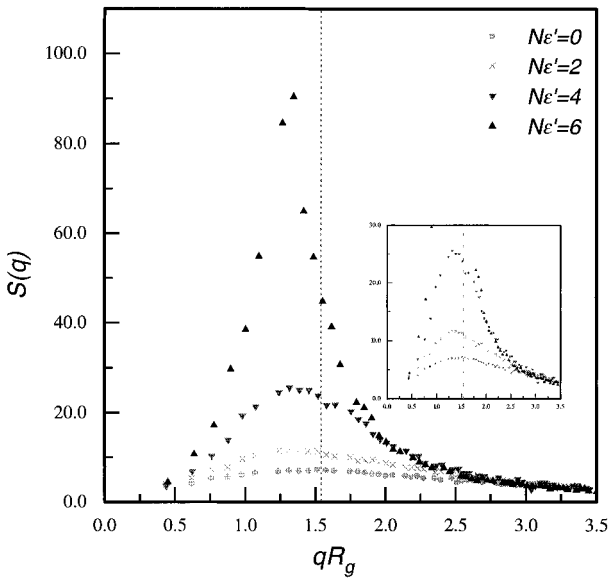

Figure 9. Structure factor $S(q)$ as a function of qR_g for $f = 0.3125$ and different values of $N\epsilon'$. Dashed line represents q^*R_g value according to RPA. Inset shows an enhanced vertical scale to more clearly indicate peak position in the low-energy results.

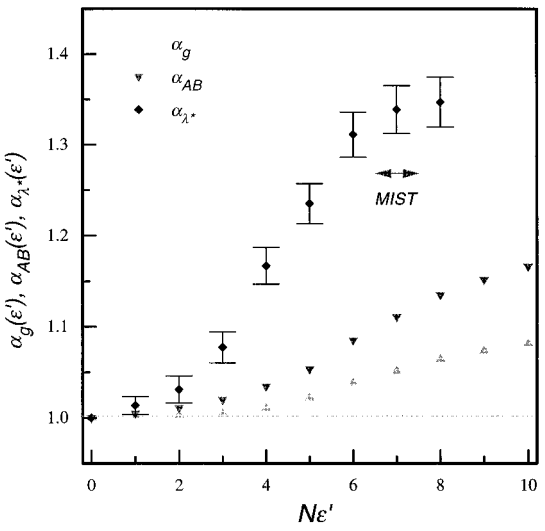

Figure 10. Expansion factors α_g, α_{AB}, and α_{λ^*} as a function of $N\epsilon'$ for $f = 0.375$.

Figures 10 and 11 present the plots of α_g, α_{AB}, and α_{λ^*} vs $N\epsilon'$ for $f = 0.375$ and $f = 0.3125$. Here, α_{λ^*} is defined as

$$\alpha_{\lambda^*}(\epsilon') = \lambda^*(\epsilon')/\lambda^*(\epsilon' = 0) \tag{31}$$

Both figures show that the coils are stretched gradually but more rapidly than the expansion of the radii of gyration. It is noteworthy that α_{λ^*} increases more rapidly than either α_g and α_{AB}. As pointed out by Fried and Binder[16] for pure diblock copolymer systems, this results implies that λ^* is not an intrinsic length scale of individual copolymers such as the radius of gyration. It is more likely that λ^* represents a local segregation of monomers with contributions coming from many copolymers. Rather than an individual length scale such as R_g, the relevant length seems to be a collective length.

To investigate the contribution of the short and the long blocks of A (or B) to the concentration profile of A

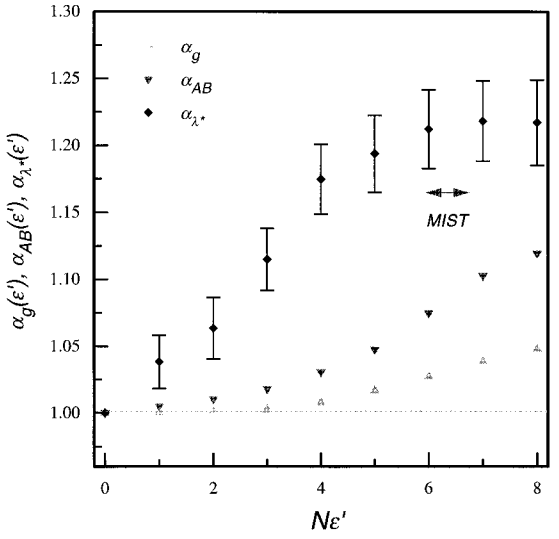

Figure 11. Expansion factors α_g, α_{AB}, and α_{λ^*} as a function of $N\epsilon'$ for $f = 0.3125$.

segment at MIST, we calculated the quantities defined as

$$S_{A1}(\vec{q}) = L^{-3}\langle\sum_{i,j} e^{i\vec{q}\cdot(\vec{r}_i-\vec{r}_j)}\psi_{A1}(\vec{r}_i)\psi_{A1}(\vec{r}_j)\rangle \quad (32)$$

$$S_{A2}(\vec{q}) = L^{-3}\langle\sum_{i,j} e^{i\vec{q}\cdot(\vec{r}_i-\vec{r}_j)}\psi_{A2}(\vec{r}_i)\psi_{A2}(\vec{r}_j)\rangle \quad (33)$$

$$S_{A1,A2}(\vec{q}) = L^{-3}\langle\sum_{i,j} e^{i\vec{q}\cdot(\vec{r}_i-\vec{r}_j)}\psi_{A1}(\vec{r}_i)\psi_{A2}(\vec{r}_j)\rangle \quad (34)$$

where the subscripts A1 and A2 stand for A segments in copolymers 1 and 2 so that A1 corresponds to an A segment in the short A block and A2 corresponds to an A segment in the long A block. The occupation variable, $\psi_{Ak}(\vec{r}_i)$ is defined by $\phi_{Ak}(\vec{r}_i) - \langle\phi_{Ak}\rangle$ having the value of $1 - \langle\phi_{Ak}\rangle$ or $-\langle\phi_{Ak}\rangle$ in the lattice system. From the structure factor of the cross product, $S_{A1,A2}(\vec{q})$, we calculated the phase difference, $\Delta\varphi$, between the profiles of A1 and A2 as

$$S_{A1,A2}(\vec{q}) = \langle X(\vec{q})\rangle + i\langle Y(\vec{q})\rangle \quad (35)$$

$$\Delta\varphi = \cos^{-1}[\langle X(\vec{q})\rangle/R(\vec{q})] \quad (36)$$

where $R(\vec{q})$ is the modulus of $S_{A1,A2}(\vec{q})$.

Figures 12 and 13 show the spherically averaged values of S_{A1} and S_{A2} vs qR_g for $f = 0.375$, $N\epsilon' = 7$ (Figure 12) and $f = 0.3125$, $N\epsilon' = 6.5$ (Figure 13), where the values of $N\epsilon'$ for the given fraction are supposed to be the value at MIST as determined by calculating the equilibrium time correlation function.[16] For $f = 0.375$, the peak positions of S_{A1} as well as S_{A2} coincide with the peak position of S in Figure 8. For $f = 0.3125$, the peak position of S_{A1} is rather uncertain in comparison with that of S_{A2}, which has a well-defined peak coinciding with the peak in Figure 9. This result agrees with our theoretical prediction presented in Figure 3, which demonstrates that the amplitude of the concentration profile of A1 decreases as the asymmetry of the block copolymer increases and vanishes at $f \cong 0.307$.

Ultimately, the amplitude ratio between the profiles of A1 and A2 is predicted to become negative below $f \cong 0.307$, which implies that the profiles are out of phase already before the macrophase separation sets in at $f \cong 0.211325$. These theoretical predictions are corroborated by our simulations as shown in Figures 14–16, where results for three different fractions, $f = 0.375$, 0.3125, and 0.25, are presented. In these figures, $S(\vec{q})$ (not spherically averaged) is plotted as a function of cos($\Delta\phi$). Every point corresponds to a different wave vector $\vec{q} = (q_1,q_2,q_3)$ from the set

$$(q_1,q_2,q_3) \in \frac{2\pi}{L}(n_x,n_y,n_z); \quad \frac{2\pi}{L}\sqrt{n_x^2 + n_y^2 + n_z^2} \le 1.25 \quad (37)$$

For $f = 0.375$ (Figure 14), most of the well-developed structure factors are found near $\Delta\phi = 0$, which implies that the A1 segment profile is in phase with the A2 profile. This situation is reversed as f decreases. For $f = 0.3125$, which is close to $f \cong 0.307$, our simulation result shows that the dominant $S(\vec{q})$ are rather randomly distributed in the plot of $S(\vec{q})$ vs $\Delta\phi$. When the asymmetry increases as much as $f < 0.307$, like the case of $f = 0.25$ presented in Figure 16, the plot becomes rather biased toward $\Delta\phi = \pi$ so that the short A blocks are pulled by the connected long B block into the B-rich

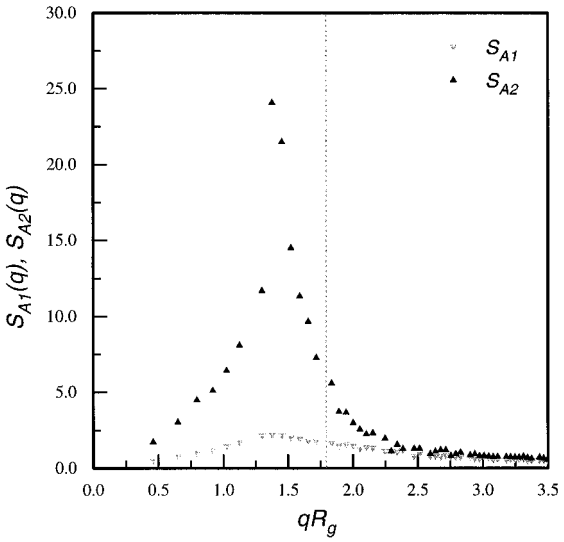

Figure 12. Structure factors of short, $S_{A1}(q)$, and long, $S_{A2}(q)$, A-blocks as a function of qR_g for $f = 0.375$ and $N\epsilon' = 7$. Dashed line represents RPA prediction of q^*R_g.

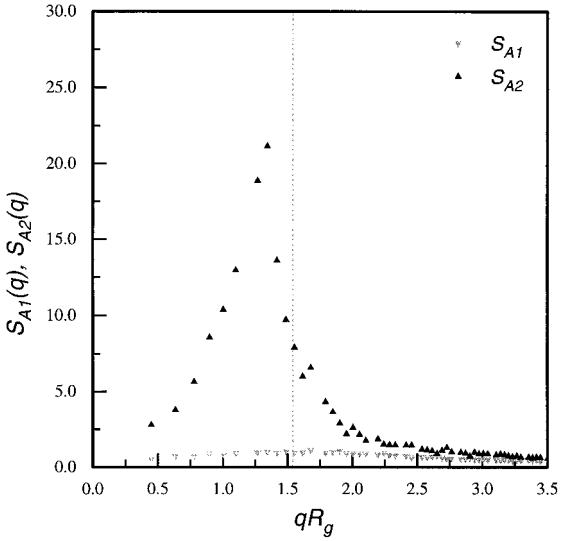

Figure 13. Structure factors of short, $S_{A1}(q)$, and long, $S_{A2}(q)$, A-blocks as a function of qR_g for $f = 0.3125$ and $N\epsilon' = 6.5$. Dashed line represents RPA prediction of q^*R_g.

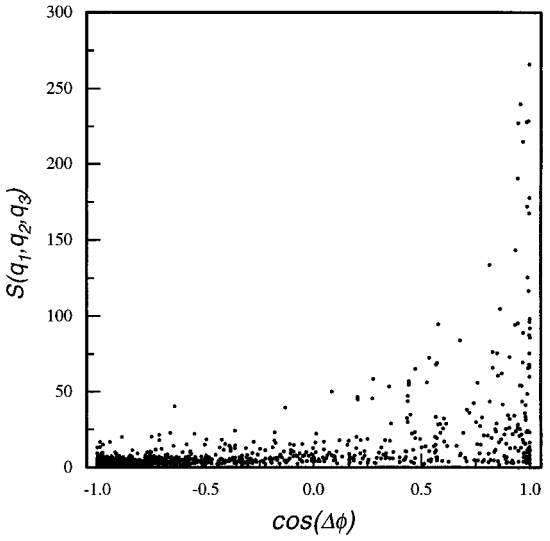

Figure 14. Value of the structure factor $S(q_1,q_2,q_3)$ for a large set of (q_1,q_2,q_3) values given by eq 37. The horizontal axis presents the corresponding $\cos(\Delta\varphi)$, where $\Delta\varphi$ is the angle between the short and long A-block profiles (fluctuations) defined in eqs 35 and 36. $f = 0.375$ and $N\epsilon' = 7$.

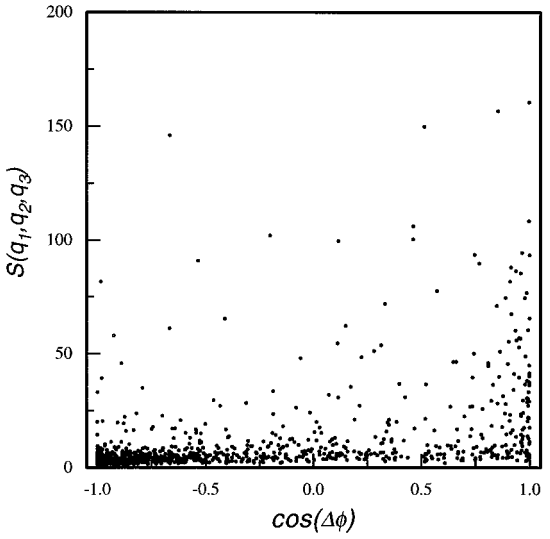

Figure 15. As in Figure 14, but now for $f = 0.3125$ and $N\epsilon' = 6.5$.

phase. In particular, the highest values of $S(\vec{q})$ corresponding to $q \cong q^*$ occur at $\Delta\phi = \pi$.

Based on these results, a very schematic morphology (more like the strong segregation regime) for three different regimes is given in Figure 17. In regime I, where $f > 0.307$, the chains nearly behave like the chains in the symmetric pure diblock copolymer system. The wavelength is not much different from the wavelength in the symmetric pure diblock copolymer system and becomes even slightly bigger as the asymmetry increases. In regime II, where $0.211325 < f < 0.307$, the short A (or B) block is out of phase with the long A (or B) block since the elastic energy which should be balanced by avoiding unfavorable contacts is too high. Subsequently, the wavelength starts to increase very rapidly. Then finally, macrophase separation sets in for $f < 0.211325$ (regime III).

Figure 18 presents the phase diagram for the system investigated. Even though our estimation of the transition temperature by the numerical simulations, particularly the values for the MISTs, has a rather large uncertainty, the curve deviates considerably from the

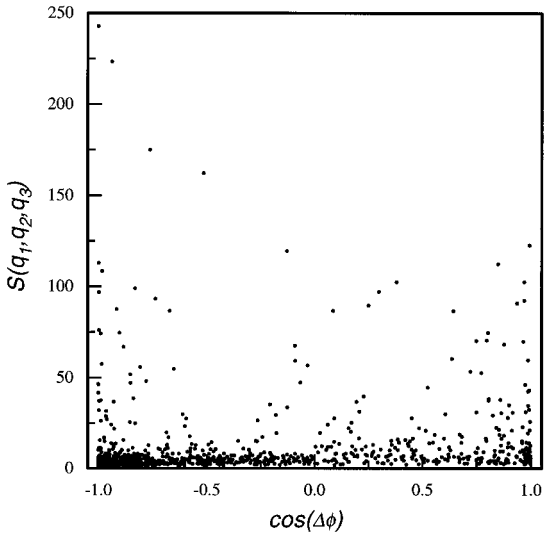

Figure 16. As in Figure 14, but now for $f = 0.25$ and $N\epsilon' = 5.5$.

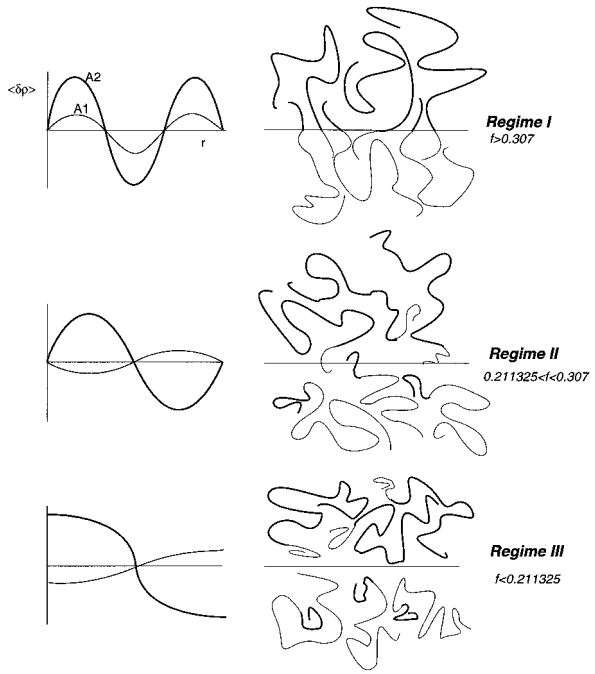

Figure 17. Schematic morphology of $A_fB_{1-f}/A_{1-f}B_f$ symmetric diblock copolymer blends.

theoretically predicted curve. The higher value of the interaction parameter at the transition for the simulation results has been demonstrated to result at least partly from the stretching/polarization of the molecules in the homogeneous state long before the actual transition. Another part might be due to the rather small chain length simulated here. However, Hartree corrections for this system, like the results by Fredrickson and Helfand for the pure diblock copolymer system,[34] are not available yet.

5. Summary

In this paper, we presented the results of a theoretical and numerical (computer simulation) study on a particularly simple symmetric diblock copolymer melt $A_fB_{1-f}/A_{1-f}B_f$. The theoretical analysis was based on a recently introduced many-order parameter approach. In this way, we were able to distinguish between the concentration fluctuations of identical monomers be-

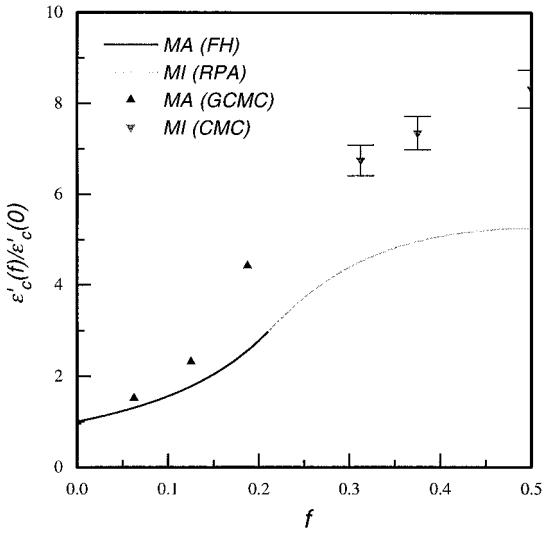

Figure 18. Phase diagram of the symmetric diblock copolymer blend $A_fB_{1-f}/A_{1-f}B_{1-f}$. MA = macrophase separation; MI = microphase separation; FH = Flory−Huggins; RPA = Random Phase Approximation; GCMC = Semi-Grand-Canonical Monte Carlo; CMC = Canonical Monte Carlo.

longing to different chains. Our system shows macrophase separation for $f < 0.211325$ and microphase separation for $0.211325 < f \leq 0.5$. The approach toward macrophase separation from the microphase-separated regime, i.e. $f \downarrow 0.211325$, is signaled not only by an increase in long period but most strikingly, by the out-of-phase behavior of the concentration fluctuations of the chemically identical segments belonging to the long and short blocks. The possibility of addressing these kinds of fluctuations details is an important asset of the multiorder parameter approach, which in turn inspired us to look for these details in the computer simulations. Clearly, many more results will soon become available along these lines.

Acknowledgment. Useful discussions with I. Ya. Erukhimovich throughout the course of this work are gratefully acknowledged.

References and Notes

(1) Legge, N. R., Holden, G., Schroeder, H. E., Eds. *Thermoplastic Elastomers*; Hanser: New York, 1992.
(2) Fredrickson, G. H.; Milner, S. T.; Leibler, L. *Macromolecules* **1992**, *25*, 6341.
(3) Sfatos, C. D.; Gutin, A. M.; Shaknovich, E. I. *Phys. Rev. E* **1995**, *51*, 4727.
(4) Angerman, H.; ten Brinke, G.; Erukhimovich, I. Ya. *Macromolecules* **1996**, *29*, 3255.
(5) Erukhimovich, I. Ya.; Dobrynin, A. V. *Macromol. Symp.* **1994**, *81*, 253.
(6) Leibler, L. *Macromolecules* **1980**, *13*, 1602.
(7) Erukhimovich, I. Ya. *Sovremennoe Sostoyanie I Problemy Statisitcheskoi Teorii Domennoi Struktury v Polimernykh Sistemakh* (The Current State and Problems of the Statistical Theory of Domain Structure in Polymer Systems), Preprint of NTsBI, Pushchino, 1985, No. T07930.
(8) Erukhimovich, I. Ya.; Khokhlov, A. R. *Polym. Sci. USSR (Engl. Transl.)* **1993**, *35*, 1522. Translated from *Vysokomol. Soedin.* **1993**, *35*, 1808.
(9) Selke, W. *Phase Transitions and Critical Phenomena*; Domb, C., Lebowitz, J. L., Eds.; Academic: New York, 1992; Vol. 15.
(10) Broseta, D.; Fredrickson, G. H. *J. Chem. Phys.* **1990**, *93*, 2927.
(11) Bates, F. S.; Wayne, M.; Lodge, T. P.; Schulz, M. F.; Matsen, M. W. *Phys. Rev. Lett.* **1995**, *75*, 4429.
(12) Shi, A.-C.; Noolandi, J. *Macromolecules* **1995**, *28*, 3103.
(13) Matsen, M. W.; Bates, F. S. *Macromolecules* **1995**, *28*, 7298.
(14) Matsen, M. W. *Phys. Rev. Lett.* **1995**, *74*, 4225; *Macromolecules* **1995**, *28*, 5765.
(15) Minchau, B.; Dünweg, B.; Binder, K. *Polym. Commun.* **1990**, *31*, 348.
(16) Fried, H.; Binder, K. *J. Chem. Phys.* **1991**, *94*, 8349.
(17) Deutsch, H.-P. *J. Stat. Phys.* **1992**, *67*, 1039.
(18) Deutsch, H. P.; Binder, K. *Macromolecules* **1992**, *25*, 6214.
(19) Burger, C.; Ruland, W.; Semenov, A. N. *Macromolecules* **1990**, *23*, 3339.
(20) ten Brinke, G.; Karasz, F. E.; MacKnight, W. J. *Macromolecules* **1983**, *16*, 1827.
(21) Sariban, A.; Binder, K. *J. Chem. Phys.* **1987**, *86*, 5859.
(22) Müller, M.; Binder, K. *Comput. Phys. Commun.* **1994**, *84*, 173.
(23) Wall, F. T.; Mandel, F. *J. Chem. Phys.* **1975**, *63*, 4592.
(24) Metropolis, N.; Rosenbluth, A. W.; Rosenbluth, M. N.; Teller, A. H.; Teller, E. *J. Chem. Phys.* **1953**, *21*, 1087.
(25) de Gennes, P.-G. *Scaling Concepts in Polymer Physics*; Cornell University Press: Ithaca, NY, 1979.
(26) Carmesin, I.; Kremer, K. *Macromolecules* **1988**, *21*, 2819.
(27) Verdier, P. H.; Stockmayer, W. H. *J. Chem. Phys.* **1962**, *36*, 227.
(28) Schwahn, D.; Mortensen, K.; Yee-Madeira, Y. *Phys. Rev. Lett.* **1987**, *58*, 1544.
(29) Bates, F. S.; Rosedale, J. H.; Stepanek, P.; Lodge, T. P.; Wiltzius, P.; Fredrickson, G. H.; Hjelm, R. P., Jr. *Phys. Rev. Lett.* **1990**, *65*, 1893.
(30) Schweizer, K. S.; Curro, J. G. *Phys. Rev. Lett.* **1987**, *58*, 246.
(31) Curro, J. G.; Schweizer, K. S. *J. Chem. Phys.* **1987**, *87*, 1842.
(32) Singh, C.; Schweizer, K. S.; Yethiraj, A. *J. Chem. Phys.* **1995**, *102*, 2187.
(33) Binder, K.; Fried, H. *Macromolecules* **1993**, *26*, 6878.
(34) Fredrickson, G. H.; Helfand, E. J. *J. Chem. Phys.* **1987**, *87*, 697.

MA9517153